



**University of
Zurich**^{UZH}

**Zurich Open Repository and
Archive**

University of Zurich
University Library
Strickhofstrasse 39
CH-8057 Zurich
www.zora.uzh.ch

Year: 2024

**In situ temperature determination using magnetic resonance spectroscopy
thermometry for noninvasive postmortem examinations**

Zoelch, Niklaus ; Heimer, Jakob ; Richter, Henning ; Luechinger, Roger ; Archibald, Jessica ; Thali, Michael J ;
Gascho, Dominic

DOI: <https://doi.org/10.1002/nbm.5171>

Posted at the Zurich Open Repository and Archive, University of Zurich

ZORA URL: <https://doi.org/10.5167/uzh-260205>

Journal Article

Published Version



The following work is licensed under a Creative Commons: Attribution-NonCommercial 4.0 International (CC BY-NC 4.0) License.



Originally published at:

Zoelch, Niklaus; Heimer, Jakob; Richter, Henning; Luechinger, Roger; Archibald, Jessica; Thali, Michael J; Gascho, Dominic (2024). In situ temperature determination using magnetic resonance spectroscopy thermometry for noninvasive postmortem examinations. *NMR in Biomedicine*:Epub ahead of print.

DOI: <https://doi.org/10.1002/nbm.5171>

RESEARCH ARTICLE

In situ temperature determination using magnetic resonance spectroscopy thermometry for noninvasive postmortem examinations

Niklaus Zoelch^{1,2}  | Jakob Heimer¹ | Henning Richter³ | Roger Luechinger⁴ |
Jessica Archibald⁵ | Michael J. Thali¹ | Dominic Gascho¹ 

¹Department of Forensic Medicine and Imaging, Institute of Forensic Medicine, University of Zurich, Zurich, Switzerland

²Department of Adult Psychiatry and Psychotherapy, Psychiatric University Hospital Zurich and University of Zurich, Zurich, Switzerland

³Clinic of Diagnostic Imaging, Vetsuisse Faculty, University of Zurich, Zurich, Switzerland

⁴Institute for Biomedical Engineering, University and ETH Zurich, Zurich, Switzerland

⁵Department of Radiology, Weill Cornell Medicine, New York, New York, USA

Correspondence

Niklaus Zoelch, Institute of Forensic Medicine, University of Zurich, Winterthurerstrasse 190/52, CH-8057 Zurich, Switzerland.
Email: niklaus.zoelch@uzh.ch

Abstract

Magnetic resonance spectroscopy (MRS) thermometry offers a noninvasive, localized method for estimating temperature by leveraging the temperature-dependent chemical shift of water relative to a temperature-stable reference metabolite under suitable calibration. Consequentially, this technique has significant potential as a tool for postmortem MR examinations in forensic medicine and pathology. In these examinations, the deceased are examined at a wide range of body temperatures, and MRS thermometry may be used for the temperature adjustment of magnetic resonance imaging (MRI) protocols or for corrections in the analysis of MRI or MRS data. However, it is not yet clear to what extent postmortem changes may influence temperature estimation with MRS thermometry. In addition, N-acetylaspartate, which is commonly used as an in vivo reference metabolite, is known to decrease with increasing postmortem interval (PMI). This study shows that lactate, which is not only present in significant amounts postmortem but also has a temperature-stable chemical shift, can serve as a suitable reference metabolite for postmortem MRS thermometry. Using lactate, temperature estimation in postmortem brain tissue of severed sheep heads was accurate up to 60 h after death, with a mean absolute error of less than 0.5°C. For this purpose, published calibrations intended for in vivo measurements were used. Although postmortem decomposition resulted in severe metabolic changes, no consistent deviations were observed between measurements with an MR-compatible temperature probe and MRS thermometry with lactate as a reference metabolite. In addition, MRS thermometry was applied to 84 deceased who underwent a MR examination as part of the legal examination. MRS thermometry provided plausible results of brain temperature in comparison with rectal temperature. Even for deceased with a PMI well above 60 h, MRS thermometry still provided reliable readings. The results show a good suitability of MRS thermometry for postmortem examinations in forensic medicine.

Abbreviations: CSF, cerebrospinal fluid; FTMA, free trimethylammonium; GM, gray matter; MAE, mean absolute error; MRS, magnetic resonance spectroscopy; MSE, mean squared error; NAA, N-acetylaspartate; PMI, postmortem interval; SNR, signal-to-noise ratio; WM, white matter.

This is an open access article under the terms of the [Creative Commons Attribution-NonCommercial](https://creativecommons.org/licenses/by-nc/4.0/) License, which permits use, distribution and reproduction in any medium, provided the original work is properly cited and is not used for commercial purposes.

© 2024 The Authors. *NMR in Biomedicine* published by John Wiley & Sons Ltd.

KEYWORDS

MRS, postmortem, temperature, thermometry, virtopsy, virtual autopsy

1 | INTRODUCTION

The advent of magnetic resonance imaging (MRI) and magnetic resonance spectroscopy (MRS) in forensic medicine has facilitated noninvasive examinations of the deceased.^{1,2} However, a challenge arises from the varying body temperatures when it comes to data interpretation and analysis.^{3–6} This is due to temperature dependence on various MR parameters, such as longitudinal and transversal relaxation times,^{7,8} thermal equilibrium magnetization,^{9,10} and chemical shifts.^{11,12} Therefore, in principle, the temperature at the measured body region is needed to either adapt the measurement protocol or to correct the outcome in the analysis. At the Institute of Forensic Medicine of the University of Zurich, for example, the body temperature of the deceased during examination ranges from 4 to 37°C. Although the temperature can already be different at the time of death (e.g., because of fever or hypothermia), it is primarily determined by passive adaptation to the ambient temperature until the corpse is found and the active cooling in cooling chambers afterwards.¹³ To correct for the influence of temperature on the MR measurement, it would be simplest to use the rectally measured body temperature, which is also routinely collected in forensic medicine to estimate the time of death.^{14,15} But unfortunately, the postmortem body temperature inaccurately reflects temperature in other body regions such as the head, as opposed to in vivo measurements. In postmortem examinations, significant temperature differences of several degrees can be observed in the body owing to distinct cooling curves in various body regions.¹⁶ Such variations can be further exacerbated in cases of severe open injuries involving nonintact bodies or under unique circumstances, such as incidents involving the corpse partially being submerged in water. For a head MR examination, directly measuring tissue temperature with a thermometer, such as through the nasal passage and the cribriform plate, is impractical and poses a risk of potential damage that may influence the forensic evaluations.¹⁷ Hence, noninvasive methods are required. Recently, a study demonstrated a model for predicting temperature in the longitudinal fissure using data like forehead temperature, ambient temperature, sex, and humidity.¹⁸ The generalizability of this model, developed from a relatively small sample size ($n = 16$), remains uncertain. An alternative approach for noninvasive postmortem temperature assessment is leveraging the temperature dependence of MR parameters.⁸ For instance, previous efforts have been made to estimate brain core temperature in the deceased by examining the temperature-dependent diffusion coefficient in the cerebral spinal fluid (CSF).³

MRS thermometry exploits the fact that the proton chemical shift of water in the liquid phase is linearly dependent on the temperature, with a coefficient of approximately -0.01 parts-per-million (ppm)/°C.¹² This dependency is primarily caused by the temperature dependence of the fraction and the nature of hydrogen bonds in water, which affects the electronic environment of the protons within the water molecule and therefore the chemical shift, as nicely illustrated by Kuroda.¹⁹ What MRS thermometry adds is the ability to measure reference peaks with a temperature-stable chemical shift, which can be used to eliminate changes in the strength of the magnetic flux density (B_0) experienced by the reference compound and water. Thus, based on the frequency difference between water and the reference peak ($\Delta_{(H_2O-ref)}$), estimating the local temperature^{20,21} is possible. This is an advantage compared with MRI-based techniques exploiting the temperature dependence of the chemical shift of water, by which relative temperature changes can be detected.^{8,19}

A calibration is required to convert $\Delta_{(H_2O-ref)}$ into a temperature estimation (T_{MRS}). The calibration is created by measuring $\Delta_{(H_2O-ref)}$ at a series of known temperatures. By classical or inverse methods, a calibration function with slope and intercept is calculated.²² A large number of calibrations for MRS thermometry have been published,^{20,21,23–32} predominantly utilizing N-acetylaspartate (NAA) as the reference peak, and occasionally for creatine^{25,26,31,32} or choline,³¹ determined either in animals or in phantom measurements. Despite this, there is little consensus on the reported slope and intercept values for the temperature calibration,³¹ probably because of the influence of other factors than temperature on the observed $\Delta_{(H_2O-ref)}$. Possible nontemperature-based factors include changes in the electronic environment of the involved nuclei due to changes in ionic concentration,^{27,29,33} protein concentration,^{27,29,34} pH,^{21,27} and differences of local magnetic susceptibility on a microscopic level or differences of tissue magnetic architecture.^{31,35,36} Discrepancies in nontemperature-related factors between the calibration measurements and the examined tissue can lead to inaccuracies in the calculated temperature. This is why a temperature determined through MRS thermometry is often referred to as “apparent temperature.” In measurements of the deceased in the forensic medical setting, postmortem changes play an important role in addition to intraindividual differences that already existed before death. After death and the accompanying depletion of oxygen reserves, anaerobic glycolysis causes the pH in cytosol and extracellular fluid to decrease sharply (i.e., down to 6.3) in the first 9 h after death³⁷ (Band 1, Chapter 2.1). As ATP deficiency progresses, membrane transport mechanisms become slack and ionic concentration differences between cell interior and extracellular fluid equalize. Degradation of matter by endogenous enzymes (in the course of autolysis) leads to cleavage of proteins and consequent changes in protein content. As bacteria invade the tissue, catabolic autolysis is increasingly masked by putrefaction (in the absence of oxygen) or decomposition processes (in the presence of oxygen)³⁷ (Band 1, Chapter 2.2). These postmortem changes can impact the measured $\Delta_{(H_2O-NAA)}$ and consequentially T_{MRS} , potentially necessitating different calibrations rendering accurate temperature measurement with MRS thermometry nearly impossible. In addition, the typical reference metabolite for MRS thermometry in the brain, the NAA

peak, demonstrates a marked decrease with an extended postmortem interval (PMI).^{3,38} Consequently, NAA cannot be considered a universally reliable reference metabolite for postmortem MRS thermometry. A more suitable reference metabolite might be lactate, for several reasons. First, the lactate signal increases rapidly within minutes after death and is readily detectable. Second, research has demonstrated that the methyl proton chemical shift of lactate remains insensitive to changes in temperature and pH in the range of 5.94 to 7.80.³⁹

In the current study, our primary objective is to assess the viability of noninvasive MRS thermometry for on-site temperature estimation within brain tissue during postmortem examinations of the deceased.

For this purpose, we make use of published calibrations that have been measured for in vivo applications. To prepare for a broad range of PMI we convert calibrations determined with NAA as the reference metabolite to lactate as the reference metabolite, assuming that the difference between lactate and NAA is temperature stable. To investigate the postmortem reliability of the different calibrations, we measure three severed sheep heads over a PMI of up to 60 h, where the determined temperature can be checked with an inserted temperature probe. Subsequently, we applied the determined optimal calibration to measure T_{MRS} in situ in the brain white matter (WM) tissue of 84 deceased. We then compare these MRS-derived temperature estimates with conventional rectal temperature measurements taking into account the different cooling curves of these body parts. The goal is to establish a robust foundation for enhancing temperature-related corrections and assessments in postmortem MRI and MRS examinations.

2 | METHODS

2.1 | Temperature calibrations

Based on the collections of calibrations shown in,^{19,27,29} we collected published calibrations (Table 1) for in vivo applications since the pioneering work of Cady et al.²⁰ and Corbett et al.²¹ Most temperature calibrations available are specifically for NAA as the reference metabolite. Here, we converted the calibrations using NAA to be able to estimate the local temperature $T_{MRS,Lac}$ (in °C) using the chemical shift difference measured in ppm between water and lactate ($\Delta_{(H_2O-Lac)}$) instead:

TABLE 1 Published temperature calibrations with slope of calibration (α) and intercept (β) to obtain temperature estimates in °C.

Calibration Label	Values			Results	
	α (°C/ppm)	β (°C)	Ref.	RSME	MAE
Zhu	-103.80	313.76	25	0.515	0.417
Marshall	-100.00	303.50	24	0.553	0.446
Covaciu.cre	-94.77	193.29	26	0.594	0.460
Cady	-94.00	286.90	20	0.736	0.588
Maudsley	-102.76	310.50	31	0.757	0.649
Covaciu	-97.13	296.07	26	0.759	0.625
Zhu.cre	-101.70	204.67	25	0.890	0.711
Maudsley.cre	-102.61	206.10	31	1.005	0.809
Vescovo	-101.02	305.40	27	1.041	0.928
Verius.cre	-102.25	204.82	32	1.547	1.395
Verius	-104.75	314.97	32	1.618	1.546
Kuroda	-103.09	310.41	23	1.643	1.568
Corbett	-98.47	296.70	21	2.661	2.595
Babourina	-101.72	305.16	29	3.098	3.054
Prakash	-102.76	314.37	28	3.342	3.304
Dehkharghani	-90.91	273.73	30	4.912	4.842

Note: In total, 16 published calibrations were tested in this study. Four of these calibrations were determined for the chemical shift difference between water and creatine (denoted with .cre) and used here for the calculation of $T_{MRS,Cre}$. All others were originally determined for the chemical shift difference between water and NAA, but used in this study to estimate the local temperature $T_{MRS,Lac}$ using the chemical shift difference between water and lactate instead (see Section 2.1 for the necessary adaptations). The RMSE and the MAE are calculated within this work. The calibrations are ordered by the RMSE obtained.

Abbreviations: MAE, mean absolute error; NAA, N-acetylaspartate; RMSE, root mean squared error.

$$T_{MRS.Lac} = \alpha \cdot \Delta_{(H_2O-Lac)} + \beta + \alpha \cdot \Delta_{(Lac-NAA)} \quad (1)$$

The derivation of Equation (1) is shown in the [supporting information](#). Based on the available literature,³⁹ we assumed $\Delta_{(Lac-NAA)}$ to be constant over the measured temperature range and set $\Delta_{(Lac-NAA)}$ to -0.68791 ppm based on the values found for NAA and L(+)-lactate on GISSMO⁴⁰ (<https://gissmo.bmrbi.io>). GISSMO was used because of its extensive coverage of chemical shifts and scalar couplings across a broad spectrum of metabolites, including also those typically encountered only in postmortem investigations, which made GISSMO values our preferential choice for in situ postmortem studies. The slope α and intercept β are given by the respective calibration. In addition, we also investigated the few calibrations available for the water chemical shift relative to creatine ($\Delta_{(H_2O-Cre)}$) (see Table 1):

$$T_{MRS.Cre} = \alpha \cdot \Delta_{(H_2O-Cre)} + \beta \quad (2)$$

2.2 | Measurements in an animal model

To determine the optimal available calibration, we simultaneously recorded $\Delta_{(H_2O-Lac)}$ and $\Delta_{(H_2O-Cre)}$ in addition to the temperature using a dedicated probe in the brains of three severed sheep heads. All specimens were collected directly after the end of another animal study following euthanization during deep anesthesia with pentobarbital (Pentobarbitalum natricum, Esconarkon ad us. vet. [100–150 mg/kg BW]; Streuli Pharma AG). After confirmation of death by the absence of heartbeat and pupillary reflex, the head was severed, carefully placed in a heat-insulating box and transported to the research facility to commence the MR experiments. The preceding study was performed according to the Swiss animal welfare act (animal license number ZH234/17).

We utilized a paramedian-frontal burr hole, created in the previous animal study, to gain catheter access to the ventricle. Through this access point, we inserted a MR-suitable fiber optic temperature probe (GaAs-crystal, polyimide tip with 0.7-mm diameter, 2-m length, accuracy of relative temperature $\pm 0.2^\circ\text{C}$; provided by Rugged Monitoring, Canada) for continuous temperature recording. The probe was carefully advanced manually until a noticeable resistance was encountered, indicating that the probe had reached the level of the left thalamus. Finally, a gentle pressure was applied to securely position the probe in the tissue. To record the ambient temperature in the scanner room, a second probe was immersed in a container filled with 1 L of water. This container was stored for the whole time in the scanner room positioned outside of the bore. To ensure accuracy, both temperature probes were calibrated 30 min before each measurement session. For this purpose, the water temperature was measured with a regularly calibrated Resistance Temperature Detector (Pt100, model: HD 2307.0 with Probe TP49A [type: immersion/application field: -70°C ... $+400^\circ\text{C}$ /accuracy: $\pm 0.25^\circ\text{C}$ (-50°C ... $+350^\circ\text{C}$), $\tau = 3.5$ s]; Delta Ohm, Padova, Italy). The fiber optic temperature probe was connected to a multichannel signal conditioner (Reflex Signal Conditioner; Neoptix, Canada) and connected to a PC (Neoptix OptiLink Pro Version 1.72; Neoptix). The acquisition rate was set to 5 s. The temperature measurement commenced with both temperature probes submerged in the water container and persisted throughout the process, including when the probe was inserted in the sheep head and when the sheep's head was repositioned to the center of the scanner bore. This approach allowed for the correction of B0-dependent temperature shifts that occur when the probe is moved in or out of the scanner bore.⁴¹

MRS measurements commenced approximately 80 min (for sheep head 1), 55 min (for sheep head 2), and 50 min (for sheep head 3) postmortem. Spectra were acquired from the right hemisphere (on the opposite side of the temperature probe) on the level of the thalamus containing a mixture of WM and gray matter (GM) tissue using the parameters described below. MRS measurements were conducted almost continuously for the first 10 h until the sheep heads had almost reached room temperature. After that, we repeatedly paused for approximately 6 h before three more measurements were taken. This procedure was repeated until the spectral quality had decreased significantly due to decomposition processes. The spectral quality was deemed insufficient when it was no longer possible to discern the two methyl lactate peaks. Following the measurement, the temperature probe was reinserted into the water container, allowing us to compare the measured temperature with the output from the resistance thermometer. This check was conducted to assess possible instabilities during the long measurement time.

2.3 | MR hardware

All experiments were performed using a 3-T whole-body MRI scanner (Achieva; Philips Healthcare, Best, the Netherlands) with software version R 5.3.1. The body coil, in combination with an eight-channel phased-array receive-only head coil (Philips Healthcare), was used for signal acquisition.

2.4 | MR acquisition

Temperature estimations were based on single-voxel MRS. To allow accurate placement of the MRS voxel, a T_1 -weighted 3D Turbo-Field-Echo sequence (repetition time [TR] = 9.4 ms, echo time [TE] = 4.6 ms) with an acquisition voxel size of $1.5 \times 1.5 \times 2 \text{ mm}^3$ over 140 slices, was conducted. Spectra were obtained with single-voxel PRESS localization (TR: 2288 ms, TE: 30 ms, readout duration 512 ms, bandwidth 4000 Hz) with variable power and optimized relaxation delays (VAPOR) water suppression⁴² (140-Hz width) and a nominal voxel size of $16 \times 16 \times 16 \text{ mm}^3$. The transmitter frequency of the radiofrequency pulses used for localization was set to 2.02 ppm and six selective saturation pulses were applied to reduce the chemical shift displacement artifact for metabolites in the chemical shift range from myo-inositol to lactate, which reduced the voxel size to approximately $12 \times 13 \times 12 \text{ mm}^3$ (AP \times RL \times FH). In total, 192 excitations were collected for each spectrum (scan time: 7 min 33 s). The acquisition of the spectra was divided into three equal blocks of 64 signal averages. At the beginning of each block, a water-unsuppressed spectrum was acquired. The detected water signals were used for eddy current correction⁴³ and the first of them to measure $T_{MRS,Lac}$ and $T_{MRS,Cre}$. Prior to MRS data collection, shimming was adjusted up to second order (pencil beam auto) and radiofrequency power was locally optimized.⁴⁴ The start of the MRS scan was noted as the time of the temperature measurement.

2.5 | Data analysis

To determine the chemical shift of water, lactate, and creatine, the .raw/.lab data were processed using MRRecon (Gyrottools; Zurich, Switzerland) and Matlab (R2020b). Preprocessing before further analysis included coil combination and eddy current correction of the metabolite and the water-unsuppressed signal. In addition, a 1-Hz Gaussian filter was applied before 8-fold zero-filling and Fourier transform. With that, the frequency spacing between points in the spectrum was 0.24 Hz or 0.0019 ppm.

To automatically calculate the frequency differences between water and the corresponding reference metabolite in the postmortem spectra, where a high variability in peak amplitudes is observed, we identified the methyl peaks of lactate in several steps. As is common practice in in vivo studies, we first converted the frequencies to ppm and set the center frequency to be 4.68 ppm. As a result, depending on the temperature, the metabolite peaks are not observed at the frequencies expected from tabulated values. Next, we used “findpeaks” in Matlab with the “MinPeakProminence” (MPP) option set to four times the standard deviation of the noise in the spectrum. With this, the found peaks are guaranteed to have a vertical drop of more than MPP from the peak on both sides. In addition, all peaks below the mean of all peak heights in the upfield spectrum were discarded. In this way, the first two remaining peaks above 1 ppm were the methyl peaks of lactate. The mean of these two peaks' positions was used as estimation of the chemical shift of lactate. Based on the chemical shift of lactate, the chemical shifts of the methyl peaks of creatine and NAA and the main peak of myo-inositol were determined by selecting found peaks around their expected values ± 0.07 ppm. The chemical shift of water was determined by searching the position of the maximum in the water unsuppressed spectrum. All measurements where this automatic procedure did not work were excluded. To assess the quality of the spectra, the signal-to-noise ratio (SNR) of the creatine peak and the lactate peak were determined, as well as the full width at half maximum (FWHM) of the water peak. All these values were calculated based on the implementation given in FID-A.⁴⁵

Based on the determined chemical shift differences, $T_{MRS,Lac}$ and $T_{MRS,Cre}$ were determined using the above equations and calibrations (Table 1) and compared with the temperature simultaneously measured with the inserted probe (T_{probe}). The mean absolute error (MAE) and root mean squared error (RMSE) were calculated to express average error for each calibration.

2.6 | Measurements in the deceased

The optimal temperature calibration determined during the animal study was subsequently applied in 84 deceased as part of forensic judicial investigations. Ethical approval was waived by the responsible ethics committee of the Canton of Zurich (waiver number 2015-0686). As part of the forensic examination, a PMI range of each deceased was estimated as part of the legal inspection at the location of death. Following the legal inspection, the deceased was transported to the institute and stored at 7°C until the MR measurement took place. For each deceased, we calculated the PMI at the time of arrival at the institute ($PMI_{arrival}$) and the PMI at the time of the MRS measurement (PMI_{MRS}). These calculations were based on the mean value of the previously estimated PMI range and the time elapsed since the legal inspection. We utilized the difference between PMI_{MRS} and $PMI_{arrival}$ as an estimate of the cooling time at 7°C.

MRS spectra were acquired from WM tissue of the left frontal lobe on the border to the parietal lobe using the T_1 -weighted image for planning. The voxel size was larger (nominal $35 \times 20 \times 15 \text{ mm}^3$, reduced by saturation pulses to $28 \times 18 \times 12 \text{ mm}^3$), TE was shorter (28 ms), and five blocks of 64 signal averages were recorded (a total of 320 averages per spectrum). Otherwise, the settings were the same as for the measurements in the sheep heads. The analysis of the data was analogous to that described above, only for deceased whose ethanol peak exceeded the lactate peak ($n = 10$), the procedure was slightly modified to look for the creatine peak first. In the deceased, however, the T_{MRS} was compared

with the rectal temperature (T_{rectal}), which was measured directly after the MR examination using a resistance temperature detector (Delta Ohm) at a minimum insertion depth of 8 cm. A one-to-one comparison of rectal and brain temperature is not meaningful because of the different cooling rates in these body regions. Yet, to gain insight into the validity of the T_{MRS} results, we plotted the difference between T_{rectal} and T_{MRS} against the estimated cooling time and compared it with a modeled difference between rectal and brain temperature based on cooling curve models^{15,16} using the following equations:

$$T_{brain.est} = \exp(-0.127 \cdot t) \cdot (T_0 - T_{ambient}) + T_{ambient}, \quad (3)$$

$$T_{rectal.est} = \exp(B \cdot t) * (T_0 - T_{ambient}) + T_{ambient}, \quad (4)$$

with $B = 0.0284 - 1.2815 * (bw^{-0.625})$ for unclothed corpses, where the body weight (bw) is given in kg.

Thus, for comparison, we calculated the difference between $T_{brain.est}$ and $T_{rectal.est}$ over time (t) for a deceased with a body weight of 60 or 80 kg, stored at an ambient temperature ($T_{ambient}$) of 7°C and with an initial temperature (T_0) of 37°C. In the given equations, the initial plateau phase with almost constant core body temperature is neglected,^{15,16} because PMI_{arrival} was more than 4 h in each case and thus the initial plateau phase was completed.

Given the wide temperature range of measurements obtained from the deceased, we conducted a thorough examination of the chemical shift difference between lactate and NAA, creatine, and myo-inositol.

3 | RESULTS

3.1 | Animal model

The course of T_{probe} and T_{MRS} , as well as the course of the MRS quality characteristics, are shown in Figure 1 for all three sheep heads measured. We successfully obtained spectra for an approximate duration of 67 h (sheep head 1), 49 h (sheep head 2), and 54 h (sheep head 3) after the time of death. The repeated measurements were discontinued if the quality was deemed insufficient, except for sheep head 1. In the case of sheep head 1, the experiments were stopped due to the unavailability of the scanner for further measurements. This resulted in a total of 117 individual measurements. All spectra allowed automatic determination of the chemical shifts and thus temperature estimation by MRS. All spectra recorded in sheep 3 over the course of the experiment are shown (Figure 2) to illustrate the observed metabolic changes. The metabolic changes are particularly pronounced in sheep heads 2 and 3. In these heads, a significant (and sudden) reduction of the creatine peak is observed and the peak of free trimethylammonium (fTMA) becomes visible. In sheep 1, fTMA is not visible and the reduction of creatine relative to lactate is less pronounced.

Across all measurements and all tested calibrations, the best agreement between T_{probe} and T_{MRS} was obtained with the calibration Zhu and lactate as the reference ($T_{MRS,Lac}(Zhu)$). The results showed that 98% of the $T_{MRS,Lac}(Zhu)$ values are within $\pm 1^\circ\text{C}$ of T_{probe} . For calibrations using creatine as the reference metabolite, the calibration Covaciu.cre gave the smallest RMSE. These two calibrations were used to calculate the T_{MRS} values shown in Figure 1. All calibrations compared and their MAE and RSME are listed in Table 1 according to the RSME obtained. The differences between T_{MRS} and T_{probe} are plotted in Figure 3 for all tested calibrations.

3.2 | Deceased

Two measurements were excluded due to insufficient spectral quality preventing the automatic determination of metabolite chemical shifts. The spectral quality of the remaining 82 measurements is summarized in Table 2, along with T_{rectal} , estimated brain temperature ($T_{MRS,Lac}(Zhu)$), PMI, and cooling times. The spectra are shown in Figure S1. Eighteen cadavers with a PMI_{arrival} longer than 24 h were measured, of which 10 had a PMI longer than 72 h. In 10 cases, ethanol was higher than the lactate peak. The NAA peak height was significantly lower than usual in vivo measurements and tended to decrease with longer PMI, as it is catabolized to acetate and aspartate.⁴⁶ The NAA peak was smaller than the creatine peak at around 75-h PMI_{MRS}. We did not observe the formation of fTMA or such a large increase in acetate as in two sheep heads in any human cadaver. In Figure 4, the measured differences between T_{rectal} and $T_{MRS,Lac}(Zhu)$ are compared with the differences calculated according to the model (Equations 3 and 4).

The measured chemical shift differences between lactate and NAA, creatine, and myo-inositol as a function of temperature ($T_{MRS,Lac}(Zhu)$) are shown in Figure 5. Differences between NAA and lactate for measurements with a smaller NAA peak than creatine were excluded because of the large uncertainty in the determination of the chemical shift difference. For the difference between lactate and creatine a slight temperature dependence is seen, while the other differences appear stable over the whole temperature range. A linear regression was used to test whether

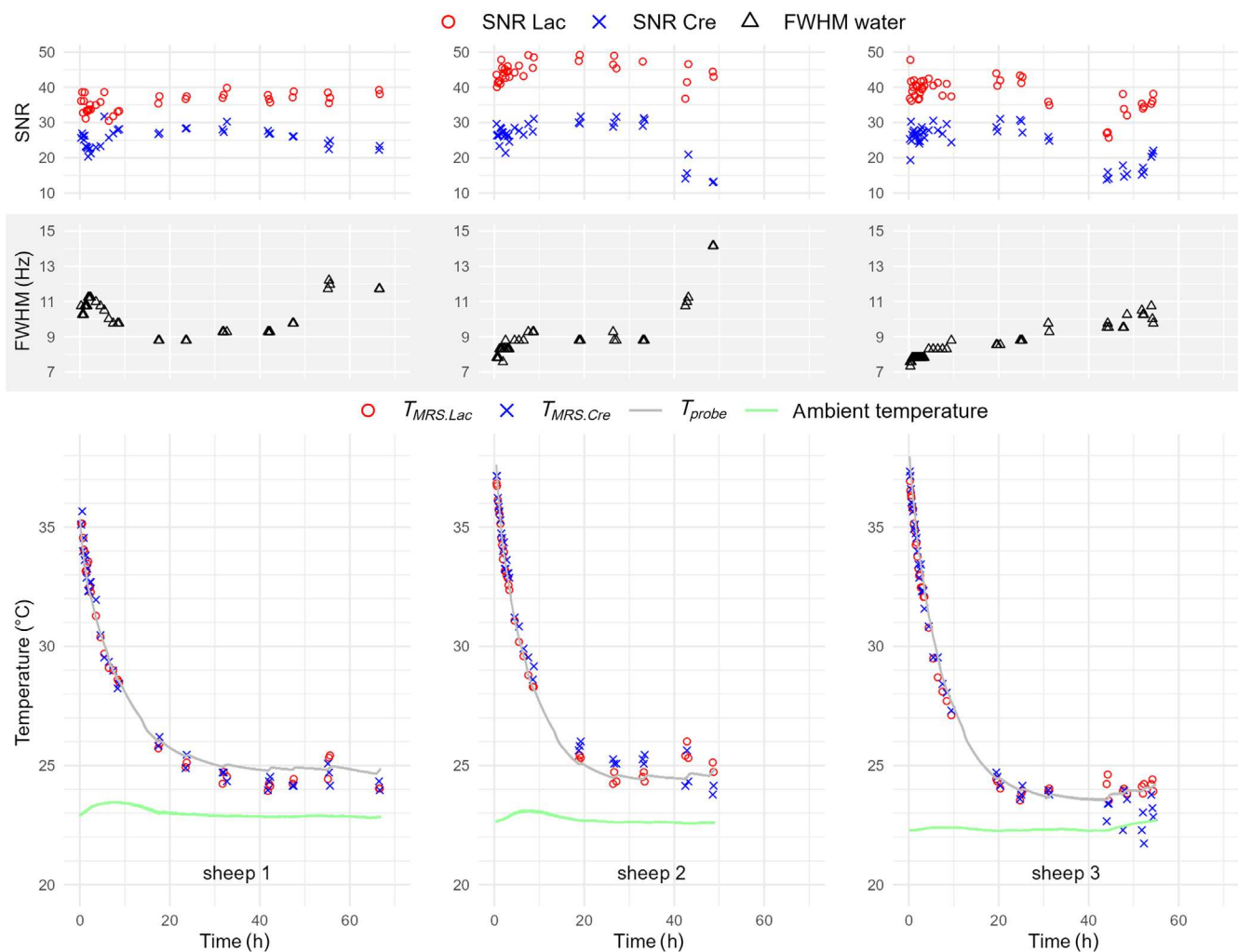


FIGURE 1 Temperature measurements in sheep brain. Bottom row: the continuously measured T_{probe} (gray) and ambient temperature (green) are shown together with the magnetic resonance spectroscopy (MRS) thermometry results. Red circles show the $T_{MRS,Lac}$ determined with the Zhu calibration and blue crosses show the $T_{MRS,Cre}$ using Covaciu.cre calibration (see Table 1 for details). Middle and top rows: the time course of the full width at half maximum (FWHM) of water and the signal-to-noise ratio (SNR) measured for lactate (Lac) and creatine (Cre). The large uncertainty in the determination of the SNR in sheep 2 shortly after 40 h is due to insufficient water suppression and the associated influence on the baseline.

the chemical shift difference between lactate and creatine was associated with brain temperature ($T_{MRS,Lac}(Zhu)$). The overall regression was statistically significant ($R^2 = 0.4193$, $F(1, 80) = 57.76$, $p = 4.897e-11$) and revealed an increase in chemical shift difference between lactate and creatine of ~ 0.33 parts-per-billion (ppb)/°C with increasing temperature ($\beta = 3.346e-01$, $p = 4.9e-11$). The creatine peak shifts towards the lactate peak with decreasing temperature.

4 | DISCUSSION

This study illustrates the suitable application of brain MRS thermometry for temperature estimation in deceased across a long PMI and thus different degrees of postmortem changes. MRS thermometry provides an easy-to-use means of noninvasive temperature estimation at the desired location and could form the basis for correcting temperature effects in MR measurements in forensic medicine and pathology. Here, we adopted published calibrations originally determined for in vivo use. Utilizing lactate as a reference peak and the calibration of Zhu et al.,²⁵ in severed sheep heads, we demonstrate reliable temperature measurements with MRS thermometry up to 60 h after death, achieving a MAE of less than 0.5°C. Also, in the deceased examined, plausible temperature measurements result, even when the estimated PMI exceeded 60 h. These findings highlight the potential utility of MRS thermometry as a valuable tool in postmortem investigations, enabling accurate temperature

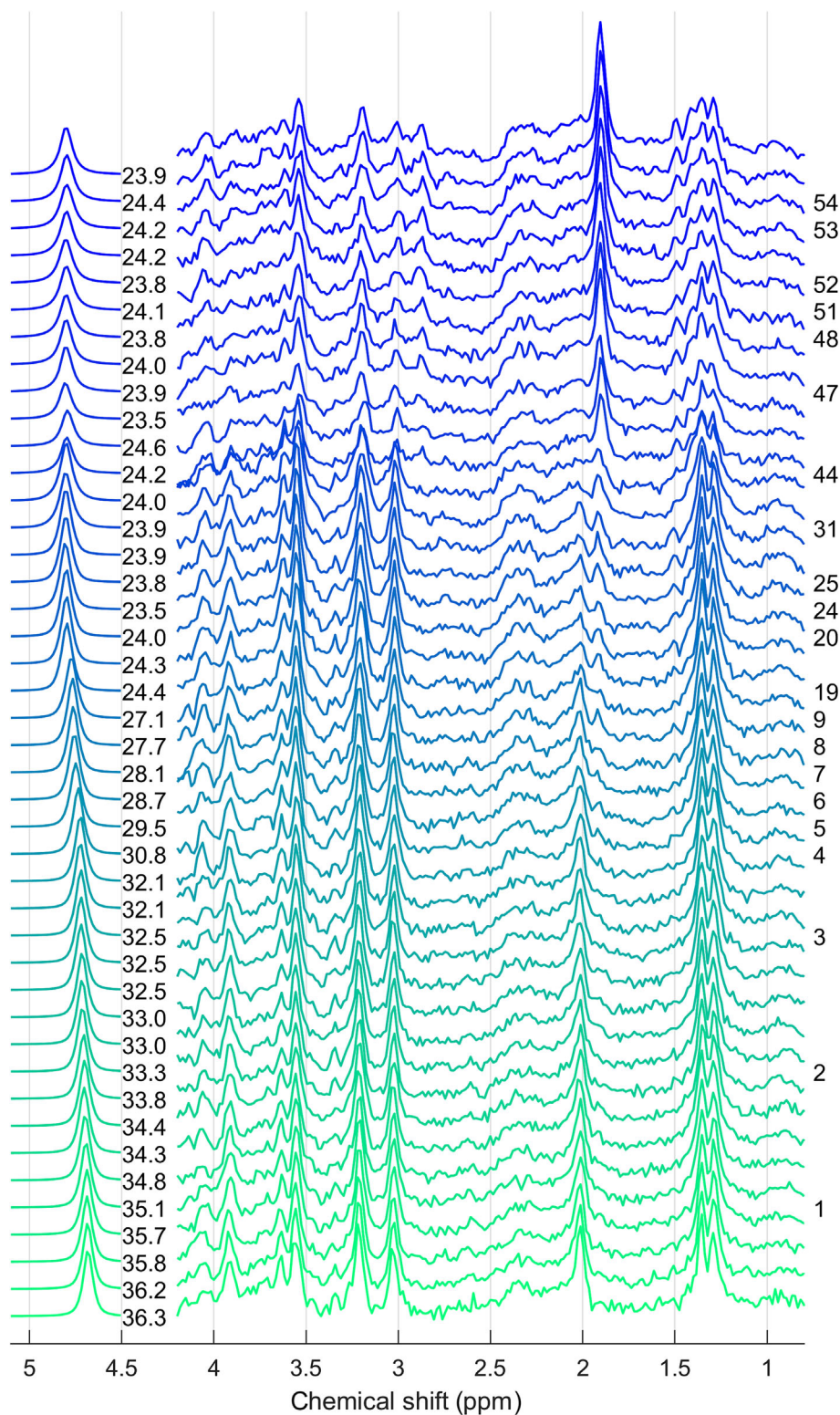


FIGURE 2 All measured spectra in sheep head 3 from the beginning (bottom) to the end (top) of the experiment. The water peak from the water-unsuppressed scan and the metabolite spectrum are shown together; the water peak is scaled accordingly. $T_{MRS,Lac}(Zhu)$ is given in the gap between the water peak and metabolite spectrum. On the right margin, the duration of the experiment is given in hours. After 40 h, with the disappearance of the NAA peak, a steep decrease of the creatine signal is visible; at 2.86 ppm, the peak of fTMA becomes visible and acetate increases strongly at 1.91 ppm. Alanine to the left of the lactate peak becomes more and more visible. All spectra are shifted such that the center of the methyl peaks of lactate appear at 1.318 ppm. fTMA, free trimethylammonium; NAA, N-acetylaspartate.

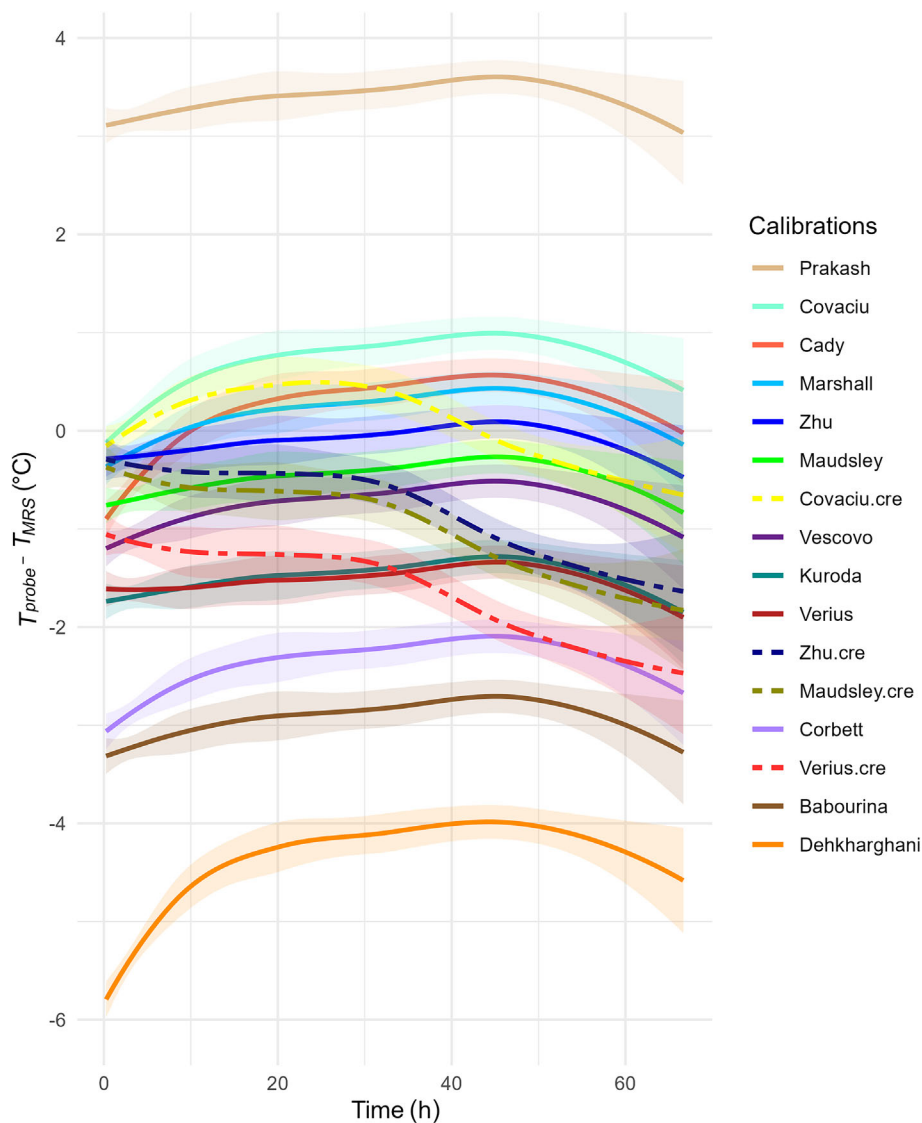


FIGURE 3 Progression of the difference between T_{probe} and T_{MRS} using all tested calibrations (Table 1) observed in the sheep head experiments. The lines show the smoothing line with the 95% confidence level interval as band.

assessment in cases with short to prolonged PMIs. Additionally, the method's adaptability for use in diverse postmortem scenarios signifies its potential for enhancing the precision and reliability of MR measurements in forensic contexts.

4.1 | Animal model

For $T_{MRS,Lac}$ and calibrations with α of the order of -103°C/ppm (Zhu, Maudsley, Verius, Kuroda), the mean differences between T_{probe} and $T_{MRS,Lac}$ are relatively constant over the whole experiment, that is, almost parallel to the zero line (Figure 3). By contrast, calibrations with α of approximately -100°C/ppm and smaller (Covaciu, Cady, Marshall, Corbett, Dehkharghani) result in a noticeable change in the difference in the first 20 h of the measurements, where the largest temperature changes occur. This suggests that calibrations with α of approximately -103°C/ppm provide better temperature estimates, which is in line with recent *in vivo* work using NAA as a reference.³¹ In our study, the calibration of Zhu et al.²⁵ provides the best agreement between T_{probe} and T_{MRS} (Table 1; Figure 3). This may be favored by the fact that the calibration was performed in real tissue (male Sprague Dawley rats). Nevertheless, it is important to note that our study does not provide definitive conclusions regarding the correct intercept value (β), which remains a point of contention in the literature.³¹ It is worth considering that constant errors resulting from using a separately acquired unsuppressed water peak, as recently described,⁴⁷ might also be a factor here, potentially favoring an “incorrect” β value. An effective approach to further investigate such errors could be via the use of the metabolite cycling technique, which allows

TABLE 2 Summary of the recorded temperatures, PMI, and MRS quality measures for the 82 deceased.

	Median	Min.	Max.
Temperature			
Rectal temperature (°C)	18.3	7.3	38.2
Brain temperature (°C)	12.2	5.4	32.8
PMI			
PMI _{arrival} (h)	7.8	1	436.2
PMI _{MRS} (h)	31.0	4.3	454.5
Estimated cooling time (h)	13.5	1.0	143.1
MRS quality			
SNR lactate	120	67	211
SNR creatine	95	71	136
FWHM water (Hz)	7.6	5.6	10.3

Note: Brain temperature was determined using $T_{MRS,Lac}(Zhu)$. The cooling time was estimated as the difference between the PMI at the time of arrival at the institute (PMI_{arrival}) and the PMI at the time of the MRS measurement (PMI_{MRS}). FWHM was measured using the unsuppressed water peak. Abbreviations: FWHM, full width at half maximum; MRS, magnetic resonance spectroscopy; PMI, postmortem interval; SNR, signal-to-noise ratio.

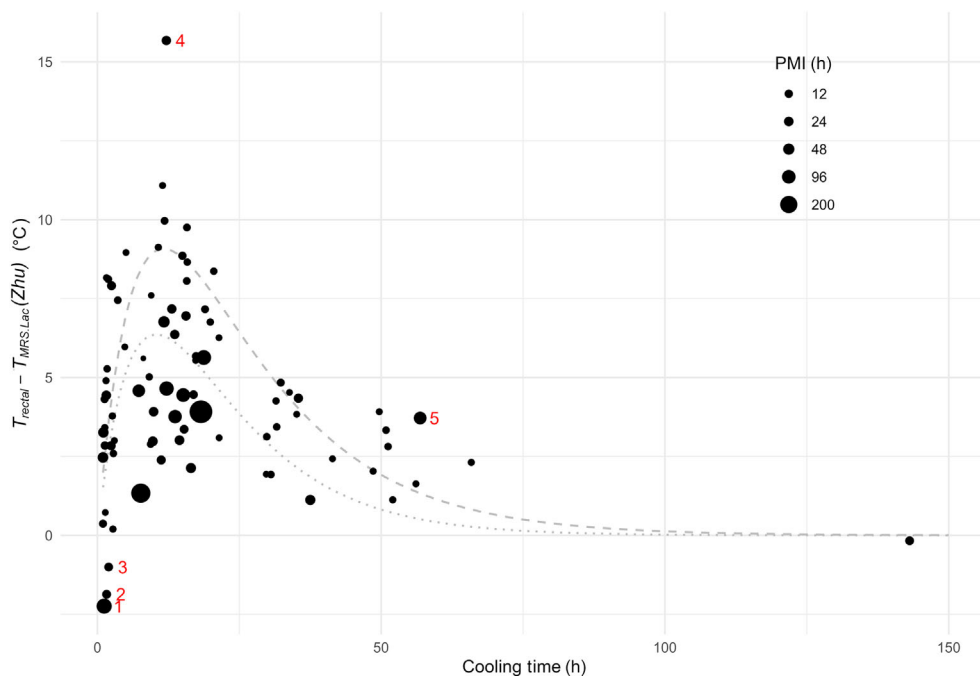


FIGURE 4 Measured differences between T_{rectal} and brain temperature estimated with $T_{MRS,Lac}(Zhu)$ as a function of cooling time measured in 82 deceased. The diameters of the dots indicate the PMI_{arrival} for each deceased. The lines show the estimated course of the difference for a body with 60 kg (dotted) and 80 kg (dashed) body weight (see Section 2.6 for details). Deceased that were examined in more detail due to the unexpected difference (see Section 4.2) are labeled with numbers (1–5). PMI, postmortem interval.

the acquisition of the metabolite spectrum and an unaltered water peak at the same time providing a means to address and mitigate potential inaccuracies. Another difficulty arises from the summand $\alpha \cdot \Delta_{(Lac-NAA)}$ in Equation (1), which originates from the conversion from NAA to lactate as the reference and contributes to the “total β .” Our conversion is based on values from GISSMO⁴⁰ ($\Delta_{(Lac-NAA)} = -0.6879$ ppm). However, Govindaraju et al.⁴⁸ reported $\Delta_{(Lac-NAA)}$ of -0.6938 ppm. Using this value results in higher temperature estimations for all calibrations (approximately $+0.6^\circ\text{C}$). And the calibration of Maudsley et al.³¹ would in this case result in smaller RMSE and MAE than the calibration of Zhu et al.²⁵ In the deceased examined in this study, we measured a mean $\Delta_{(Lac-NAA)}$ of -0.6910 ppm. In a recent conference abstract,⁴⁹ we reported slightly different RSME and MAE as in Table 1, because we used incorrectly the values of R-lactate from GISSMO, resulting in $\Delta_{(Lac-NAA)} = -0.6906$ ppm. Our study only shows that for our setup (B_0 stability, effects of eddy currents, gradient heating) at the given region in

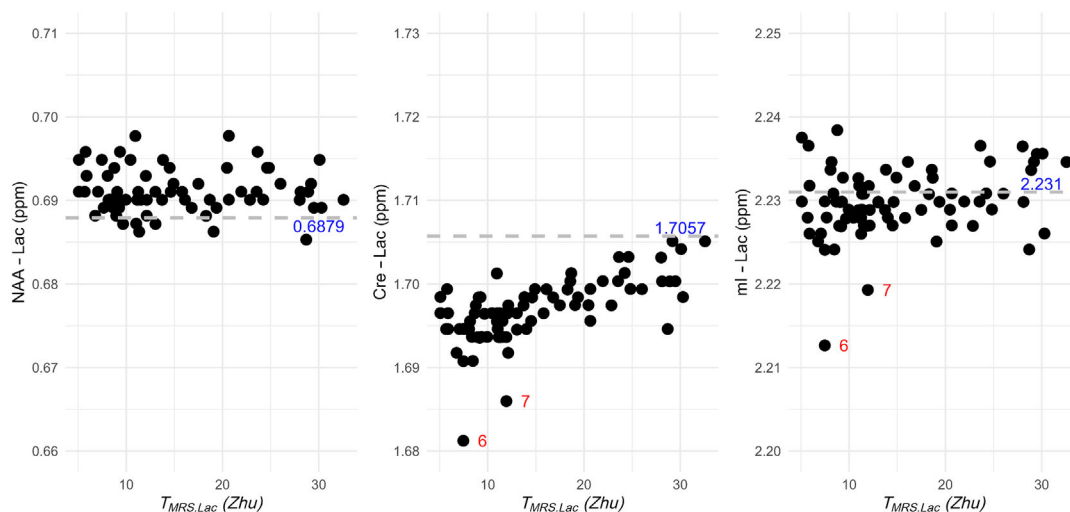


FIGURE 5 The measured chemical shift differences between lactate (Lac) and N-acetylaspartate (NAA), creatine (Cre), or myo-inositol (ml) as a function of brain temperature ($T_{MRS,Lac}(Zhu)$). The gray line indicates the expected difference based on literature values. The difference between creatine and lactate shows a clear temperature dependence of ~ 0.33 ppb/ $^{\circ}\text{C}$. The two cases with chemical shift differences that differed greatly from the others were marked and examined more closely (deceased nos. 6 and 7). The large deviations can presumably be attributed to low antemortem pH levels (see Section 4.2 for details).

the brain, by measuring the water chemical shift in a separate scan without water suppression and using the mentioned constants, the calibration from Zhu et al.²⁵ provides the best agreement between T_{probe} and T_{MRS} for our animal model. Already in another brain region, or at other GM and WM proportions in the measured voxel and thus differences in magnetic susceptibility on a microscopic level, a different calibration could be favored.

Of greater significance for the application of MRS thermometry in forensic medicine and pathology, is the observation that $T_{probe} - T_{MRS,Lac}$ changed only minimally with increasing PMI. Because of the metabolic postmortem changes mentioned (i.e., changes in the ionic content, protein content, or pH), an increasing deviation between T_{probe} and T_{MRS} with PMI might be expected. However, in the large PMI range studied here, the changes of $T_{probe} - T_{MRS,Lac}$ with increasing PMI of the three sheep heads did not reveal a clear pattern and overall $T_{probe} - T_{MRS,Lac}$ remains almost constant for longer PMI, as can be seen in Figures 1 and 3. This is despite the fact that we observe pronounced metabolic changes indicating strong postmortem changes in the severed heads (Figure 2). For example, the detection of fTMA is only observed after degradation of choline-containing compounds by anaerobic microorganisms such as gut microbes.^{50,51} Likewise, the marked decrease of creatine and increase of acetate, observed here in two sheep heads, was interpreted as the onset of bacterial decomposition.³⁸ By contrast, we observed less pronounced metabolic changes in all the measured human brains and detected no signs of bacterial invasion, even in cases with considerably longer PMI. Additionally, the linewidths from the water peak remain well below the values measured at the end of the sheep head experiments. Based on that, we believe it is plausible that reliable $T_{MRS,Lac}$ measurements, employing the same calibration, can be achieved for PMIs exceeding 60 h in intact bodies. However, this raises the question of why nontemperature-based factors do not exhibit a clear effect, even with longer PMIs. In vitro studies have indicated that the influence of ionic concentration (of the order of 0.08 ppb/mM²⁹) and protein content (2.5 ppb/protein% or smaller) on $\Delta_{(H_2O-NAA)}$ tends to be relatively small. This suggests that relatively substantial changes would be required for these factors to exert effects on T_{MRS} that surpass the uncertainties associated with estimating the resonance frequencies. Changes in microscopic magnetic susceptibility or in the distribution of magnetic susceptibility inclusions (lipids, proteins, iron, etc.) at the cellular and subcellular levels,³⁵ could potentially have a larger effect on $\Delta_{(H_2O-NAA)}$ and thus on T_{MRS} . In vivo differences in $\Delta_{(H_2O-NAA)}$ between GM and WM of 5–10 ppb³¹ and 13 ppb³⁶ have been measured and attributed to such effects. Measurable changes in the water resonance frequency due to damage to anisotropic tissue microstructures have been described in multiple sclerosis lesions.⁵² This damage disrupts the local magnetic environment, even when magnetic susceptibility remains preserved. To affect MRS thermometry, changes in microscopic magnetic susceptibility or the tissue magnetic architecture must affect the frequency of water and lactate differently. Our observations suggest that only small changes are seen in postmortem tissue in this respect. On the other hand, it is worth noting that our measurements are conducted in relatively large volumes, where certain effects could also be averaged out.

Also for $T_{MRS,Cre}$, somewhat more stable $T_{probe} - T_{MRS,Cre}$ differences are observed during the first 20 h for calibrations, with an α value of approximately -102°C/ppm compared with those with an α value of approximately -97°C/ppm (e.g., Covaciu.cre), although overall Covaciu.cre ($\alpha = -94.77^{\circ}\text{C/ppm}$) is the one with the smallest RSME and MAE. With the evident decline in the creatine signal most probably due to the onset of bacterial decomposition, an increased deviation from T_{probe} can be observed for $T_{MRS,Cre}$ on average after 40 h. This may possibly be caused by

postmortem changes, but is probably mainly due to the greatly increased uncertainty in the determination of the creatine frequency because of the smaller signal. The influence of bacterial decomposition is smaller for $T_{MRS,Lac}$ for two reasons. First, a more substantial lactate signal remains. This is agreement with the observation reported by Ith et al.³⁸ And second, with comparable signal amplitudes for lactate and creatine, the chemical shift of lactate is more accurately determined because we employed two datapoints (both peaks of the doublet) rather than relying on just one, as is the case with creatine. It was shown that by modeling the resonance as Lorentzian line shapes, the precision of frequency estimation can be improved.²⁵ For lactate, and generally for more crowded spectra, the use of linear combination model fitting (e.g., LCMModel, jMURI) is needed to improve the precision.⁴⁷

As a side note, because the temperature is affected by the multiple MR measurements, the cooling curves observed here in the sheep heads do not show normal cooling curves. In a separate experiment without MR measurements (data not shown), the sheep head cooled completely down to room temperature within 30 h. However, with MR measurements, we observed temperatures still 1.0–1.5°C above room temperature at the end of the experiments. It is worth noting that the influence of each individual measurement on this deviation is relatively small, as depicted in Figure 1.

4.2 | Deceased

Unlike with the sheep heads, direct validation of the T_{MRS} temperature was not possible here because of the invasive nature of the probe. The comparison of $T_{rectal} - T_{MRS,Lac}(Zhu)$ with differences based on empirical cooling curves serves to estimate the validity of the measured data. However, the comparison has its limitations, especially because we do not know the initial temperature T_0 at the start of cooling. This temperature is not measured in the standard procedure of the Institute of Forensic Medicine of the University of Zurich. In addition, while the cadavers are unclothed during cooling, the manner in which they are covered and placed on the ground may vary (e.g., body bag or covered by a sheet, laying on a plastic sheet), leading to slight variations in cooling rates compared with what is assumed. It is important to acknowledge that the cooling time employed is only an approximate estimate. This is because the cadavers may be removed from the cooler for brief examinations, such as for blood and urine collection. Another uncertainty comes from the fact that the rectal temperature measurement occurs at a later time point than the $T_{MRS,Lac}(Zhu)$ measurement in the brain.

Despite the limitations of this comparison, for deceased with a PMI_{arrival} of less than 24 h (Figure 4, small circles), the measured $T_{rectal} - T_{MRS,Lac}(Zhu)$ difference agrees well with the course of differences calculated according to the model (Equations 3 and 4). This is to be expected, because the initial temperatures should be relatively close to 37°C in these cases. For deceased with a longer PMI (> 48 h), the brain and body core generally have adapted to the ambient temperature at the site of discovery and the initial temperature is considerably lower in these cases. The expected differences between brain and rectal temperature are then expected to be smaller. Based on that, the accumulation of thicker points below the modeled differences in Figure 4 is convincing. The three deceased with lower rectal than brain temperature are somewhat unexpected (deceased nos. 1, 2, and 3; Figure 4). A closer examination of the case history revealed that these deceased were exposed to a cool environment for a longer period of time before transport to our institute. In two cases (deceased nos. 1 and 2), the deceased were already cooled at the hospital; in one case the corpse was lying for 12 h overnight in a river with approximately 13°C water temperature (deceased no. 3). The previous cooling caused the brain and body core to adjust to a low temperature. During the subsequent stages of transport, delivery, and MR measurement, the brain adapted more rapidly to the new ambient temperature compared with the body core. Consequently, this resulted in higher brain temperatures being measured in relation to rectal temperatures. The measured $T_{MRS,Lac}(Zhu)$ therefore are convincing. In the case of deceased no. 4 (Figure 4), with an unusually high difference between brain and rectal temperature, $T_{MRS,Lac}(Zhu)$ also seems valid, when the circumstances under which the corpse was found are taken into consideration. Deceased no. 4 was found in a bathtub with a water temperature of approximately 52°C, therefore a high initial temperature at the beginning of the cooling can be assumed. For example, an initial temperature of 50°C results in a maximum difference of 17°C between the brain and body core according to the models used. Overall, a consistent pattern emerges of brain temperatures measured in the deceased using MRS thermometry ($T_{MRS,Lac}(Zhu)$), except for deceased no. 5, for whom no explanation for the deviating result could be found. In this case, the rectal temperature was still at 9.6°C, despite the relatively long PMI and cooling time.

Although the peak-picking method for frequency measurement used herein has limitations in precision,^{25,47} analysis of the chemical shift differences between the selected metabolites still provides valuable insights. The stable $\Delta_{(NAA-Lac)}$ observed in the deceased confirms the assumptions regarding the chemical shift made for this work and confirm that lactate is a reasonable substitute for NAA as a temperature-stable reference. The temperature dependence of the chemical shift difference between lactate and creatine (~0.33 ppb/°C) is only minimally larger than might be expected based on the existing calibration measurements that have examined both creatine and NAA. Assuming a temperature-stable chemical shift for NAA, the temperature dependence for the chemical shift of creatine is 0.20 ppb/°C for Zhu, 0.23 ppb/°C for Verius, and 0.26 ppb/°C for Covaciu. The temperature dependence of the chemical shift of the methyl peak of creatine might have an influence on the fitting of postmortem data and should therefore be considered together with the reported temperature dependence of the methylene peak shift.¹¹

In two cases, striking $\Delta_{(ml-Lac)}$ and $\Delta_{(Cre-Lac)}$ values are observed (deceased nos. 6 and 7; Figure 5). In these cases the difference to the mean for $\Delta_{(ml-Lac)}$ is 0.017 and 0.01 ppm, respectively. In deceased no. 6, elevated levels of glucose and the ketone bodies acetone and β -hydroxybutyrate were seen in the MRS spectrum, while in deceased no. 7, the MRS spectrum showed above average levels of lactate. In this case a circulatory failure due to metabolic derailment with hyperglycemia/hyperacidity was suspected on the basis of high lactate values in the CSF and aqueous humor measured biochemically. All these observations taken together are suggestive of a low pH below 5.5 in the tissue, so that a part of the lactate was protonated again and present as lactic acid. Such low pH values are rather uncommon.⁵³ The protonation influences the chemical shift of the methyl protons via a change in the local electron density.⁵⁴ In the range of pH 6 to 2, the chemical shift varies from 1.31 to 1.42 ppm.⁵⁴ Roughly below a pH of 5.5, the lactate doublet shifts distinguishably closer to the water peak. In the two cases, the deviation consequently leads to an overestimation of the temperature of approximately 1.7°C (deceased no. 6) or 1°C (deceased no. 7). To correct for such effects, we recommend monitoring the difference with myo-inositol or creatine. The direct use of myo-inositol as a temperature-stable reference metabolite may not be recommended because of its highly variable postmortem concentration and the possible confusion with glycine or glycerol.⁴⁶ Whether the simultaneous use of multiple reference metabolites can improve the precision of MRS thermometry in postmortem examinations, as has been shown recently in phantom and in vivo measurements,⁵⁵ merits further investigation. While the influence of pH is troublesome for MRS thermometry with lactate as the reference, the change in lactate peak position could be interesting for forensic medicine for noninvasive detection of acidosis in the brain. For example, it could facilitate the detection of diabetic ketoacidosis.⁵⁶

The evaluated spectra were primarily acquired for the investigation of potentially case-relevant metabolites. For a temperature-only measurement at this voxel size, the scan time could be reduced to approximately 1 min to achieve a similar SNR lactate as for the measurements in the sheep heads, which is clearly beneficial for various applications, for example, for temperature correction of MR images.^{57,58} To enable even shorter measurements, it could be interesting to use a shorter TE than the 30 ms used herein. Because motion artifacts, unlike for in vivo measurements, do not play a role, sequences like image-selected in vivo spectroscopy (ISIS) or SPin ECho, full Intensity Acquired Localized (SPECIAL) could be suitable for this purpose.⁵⁹ Shorter scans are not only convenient but also crucial for enhancing the accuracy of T_{MRS} measurements by reducing errors arising from separate water and reference metabolite acquisition. In our study, T_{MRS} measurements may be subject to errors of up to approximately 0.5°C due to magnetic field drifts⁴⁷ or changes in subject temperature during the lactate measurement. The postmortem application of MRS thermometry in other tissue types, for example, muscle, might require an other reference metabolite and other calibrations. Whether the recording of temperature maps³¹ could further benefit forensic work should be investigated in studies in the future.

In conclusion, MRS thermometry utilizing lactate as a reference metabolite provides a valid temperature estimate for examinations in brains of the deceased with a PMI of up to at least 60 h, with no discernible influence of the PMI. This approach provides an easily applicable, noninvasive basis for temperature corrections of postmortem MR examinations.

ACKNOWLEDGMENTS

The authors express their gratitude to Emma Louise Kessler for her donation to the Zurich Institute of Forensic Medicine, University of Zurich, Switzerland. Open access funding provided by Universitat Zurich.

CONFLICT OF INTEREST STATEMENT

The authors have no financial conflicts of interest to disclose.

ORCID

Niklaus Zoelch  <https://orcid.org/0000-0002-9722-7783>

Dominic Gascho  <https://orcid.org/0000-0001-9004-4362>

REFERENCES

1. Thali MJ, Yen K, Schweitzer W, et al. Virtopsy, a new imaging horizon in forensic pathology: virtual autopsy by postmortem multislice computed tomography (MSCT) and magnetic resonance imaging (MRI)—a feasibility study. *J Forensic Sci.* 2003;48(2):386–403. doi:10.1520/JFS2002166
2. Heimer J, Gascho D, Thali MJ, Zoelch N. Fundamentals of in situ postmortem magnetic resonance spectroscopy of the brain in the forensic framework—a review and outlook. *Forensic Imaging.* 2022;29:200499. doi:10.1016/j.fri.2022.200499
3. Tofts PS, Jackson JS, Tozer DJ, et al. Imaging cadavers: cold FLAIR and noninvasive brain thermometry using CSF diffusion. *Magn Reson Med.* 2008;59(1):190–195. doi:10.1002/mrm.21456
4. Birkel C, Langkammer C, Haybaeck J, et al. Temperature-induced changes of magnetic resonance relaxation times in the human brain: a postmortem study. *Magn Reson Med.* 2014;71(4):1575–1580. doi:10.1002/mrm.24799
5. Ruder TD, Hatch GM, Siegenthaler L, et al. The influence of body temperature on image contrast in post mortem MRI. *Eur J Radiol.* 2012;81(6):1366–1370. doi:10.1016/j.ejrad.2011.02.062
6. Zech WD, Schwendener N, Persson A, Warntjes MJ, Jackowski C. Temperature dependence of postmortem MR quantification for soft tissue discrimination. *Eur Radiol.* 2015;25(8):2381–2389. doi:10.1007/s00330-015-3588-4
7. Bloembergen N, Purcell EM, Pound RV. Relaxation effects in nuclear magnetic resonance absorption. *Phys Ther Rev.* 1948;73(7):679–712. doi:10.1103/PhysRev.73.679

8. Rieke V, Butts Pauly K. MR thermometry. *J Magn Reson Imaging*. 2008;27(2):376-390. doi:10.1002/jmri.21265
9. Tofts P. *Quantitative MRI of the Brain: Measuring Changes Caused by Disease*. John Wiley & Sons; 2005.
10. Gultekin DH, Gore JC. Temperature dependence of nuclear magnetization and relaxation. *J Magn Reson*. 2005;172(1):133-141. doi:10.1016/j.jmr.2004.09.007
11. Wermter FC, Mitschke N, Bock C, Dreher W. Temperature dependence of (1)H NMR chemical shifts and its influence on estimated metabolite concentrations. *MAGMA*. 2017;30(6):579-590. doi:10.1007/s10334-017-0642-z
12. Hindman J. Proton resonance shift of water in the gas and liquid states. *J Chem Phys*. 1966;44(12):4582-4592. doi:10.1063/1.1726676
13. Berger C, Bauer M, Wittig H, Scheurer E, Lenz C. Post mortem brain temperature and its influence on quantitative MRI of the brain. *MAGMA*. 2022;35:375-387. doi:10.1007/s10334-021-00971-8
14. Henßge C. Todeszeitschätzungen durch die mathematische Beschreibung der rektalen Leichenabkühlung unter verschiedenen Abkühlungsbedingungen. *Z Rechtsmed*. 1981;87(3):147-178. doi:10.1007/BF00204763
15. Henssge C, Madea B. Estimation of the time since death in the early post-mortem period. *Forensic Sci Int*. 2004;144(2-3):167-175. doi:10.1016/j.forsciint.2004.04.051
16. Henssge C, Frekers R, Reinhardt A, Beckmann ER. Determination of the time of death based on simultaneous measurement of brain and rectal temperatures. *Z Rechtsmed*. 1984;93(2):123-133.
17. Naeve W, Apel D. Hirntemperatur der Leiche und Todeszeit. *Int J Leg Med*. 1973;73(2):159-169. doi:10.1007/BF01882340
18. Berger C, Bauer M, Wittig H, Gerlach K, Scheurer E, Lenz C. Investigation of post mortem brain, rectal and forehead temperature relations. *J Therm Biol*. 2023;115:103615. doi:10.1016/j.jtherbio.2023.103615
19. Kuroda K. Non-invasive MR thermography using the water proton chemical shift. *Int J Hyperthermia*. 2005;21(6):547-560. doi:10.1080/02656730500204495
20. Cady EB, D'Souza PC, Penrice J, Lorek A. The estimation of local brain temperature by in vivo ¹H magnetic resonance spectroscopy. *Magn Reson Med*. 1995;33(6):862-867. doi:10.1002/mrm.1910330620
21. Corbett RJ, Laptook AR, Tollefsbol G, Kim B. Validation of a noninvasive method to measure brain temperature in vivo using ¹H NMR spectroscopy. *J Neurochem*. 1995;64(3):1224-1230. doi:10.1046/j.1471-4159.1995.64031224.x
22. Tellinghuisen J. Inverse vs. classical calibration for small data sets. *Fresenius J Anal Chem*. 2000;368:585-588. doi:10.1007/s002160000556
23. Kuroda K, Takei N, Mulkern RV, et al. Feasibility of internally referenced brain temperature imaging with a metabolite signal. *Magn Reson Med Sci*. 2003;2(1):17-22. doi:10.2463/mrms.2.17
24. Marshall I, Karaszewski B, Wardlaw JM, et al. Measurement of regional brain temperature using proton spectroscopic imaging: validation and application to acute ischemic stroke. *Magn Reson Imaging*. 2006;24(6):699-706. doi:10.1016/j.mri.2006.02.002
25. Zhu M, Bashir A, Ackerman JJ, Yablonskiy DA. Improved calibration technique for in vivo proton MRS thermometry for brain temperature measurement. *Magn Reson Med*. 2008;60(3):536-541. doi:10.1002/mrm.21699
26. Covaciu L, Rubertsson S, Ortiz-Nieto F, Ahlstrom H, Weis J. Human brain MR spectroscopy thermometry using metabolite aqueous-solution calibrations. *J Magn Reson Imaging*. 2010;31(4):807-814. doi:10.1002/jmri.22107
27. Vescovo E, Levick A, Childs C, Machin G, Zhao S, Williams SR. High-precision calibration of MRS thermometry using validated temperature standards: effects of ionic strength and protein content on the calibration. *NMR Biomed*. 2013;26(2):213-223. doi:10.1002/nbm.2840
28. Prakash BK, Verma SK, Marchenko Y, et al. Echo planar spectroscopic imaging based temperature calibration at 7T and 3T for whole brain temperature measurement in rodents and humans. In: *Proceedings of the ISMRM Annual Meeting & Exhibition*. International Society for Magnetic Resonance in Medicine; 2014:2871.
29. Babourina-Brooks B, Simpson R, Arvanitis TN, Machin G, Peet AC, Davies NP. MRS thermometry calibration at 3 T: effects of protein, ionic concentration and magnetic field strength. *NMR Biomed*. 2015;28(7):792-800. doi:10.1002/nbm.3303
30. Dehkharghani S, Mao H, Howell L, et al. Proton resonance frequency chemical shift thermometry: experimental design and validation toward high-resolution noninvasive temperature monitoring and in vivo experience in a nonhuman primate model of acute ischemic stroke. *Am J Neuroradiol*. 2015;36(6):1128-1135. doi:10.3174/ajnr.A4241
31. Maudsley AA, Goryawala MZ, Sheriff S. Effects of tissue susceptibility on brain temperature mapping. *Neuroimage*. 2017;146:1093-1101. doi:10.1016/j.neuroimage.2016.09.062
32. Verius M, Frank F, Gizewski E, Broessner G. Magnetic resonance spectroscopy thermometry at 3 Tesla: importance of calibration measurements. *Ther Hypothermia Temp Manag*. 2019;9(2):146-155. doi:10.1089/ther.2018.0027
33. Sare E, Moynihan C, Angell C. Proton magnetic resonance chemical shifts and the hydrogen bond in concentrated aqueous electrolyte solutions. *J Phys Chem*. 1973;77(15):1869-1876. doi:10.1021/j100634a011
34. Luo J, He X, d'Avignon DA, Ackerman JJ, Yablonskiy DA. Protein-induced water ¹H MR frequency shifts: contributions from magnetic susceptibility and exchange effects. *J Magn Reson*. 2010;202(1):102-108. doi:10.1016/j.jmr.2009.10.005
35. He X, Yablonskiy DA. Biophysical mechanisms of phase contrast in gradient echo MRI. *Proc Natl Acad Sci*. 2009;106(32):13558-13563. doi:10.1073/pnas.0904899106
36. Chadzynski GL, Bender B, Groeger A, Erb M, Klose U. Tissue specific resonance frequencies of water and metabolites within the human brain. *J Magn Reson*. 2011;212(1):55-63. doi:10.1016/j.jmr.2011.06.009
37. Brinkmann B, Madea B. *Handbuch gerichtliche Medizin*. Vol. 1. Springer; 2003.
38. Ith M, Scheurer E, Kreis R, Thali M, Dirnhöfer R, Boesch C. Estimation of the postmortem interval by means of ¹H MRS of decomposing brain tissue: influence of ambient temperature. *NMR Biomed*. 2011;24(7):791-798. doi:10.1002/nbm.1623
39. Lutz N, Kuesel A, Hull W. A ¹H-NMR method for determining temperature in cell culture perfusion systems. *Magn Reson Med*. 1993;29(1):113-118. doi:10.1002/mrm.1910290120
40. Dashti H, Westler WM, Tonelli M, Wedell JR, Markley JL, Eghbalnia HR. Spin system modeling of nuclear magnetic resonance spectra for applications in metabolomics and small molecule screening. *Anal Chem*. 2017;89(22):12201-12208. doi:10.1021/acs.analchem.7b02884
41. Buchenberg WB, Dadakova T, Groebner J, Bock M, Jung B. Comparison of two fiber-optical temperature measurement systems in magnetic fields up to 9.4 Tesla. *Magn Reson Med*. 2015;73(5):2047-2051. doi:10.1002/mrm.25314

42. Tkáč I, Starčuk Z, Choi IY, Gruetter R. In vivo ^1H NMR spectroscopy of rat brain at 1 ms echo time. *Magn Reson Med*. 1999;41(4):649-656. doi:10.1002/(SICI)1522-2594(199904)41:43.0.CO;2-G
43. Klose U. In vivo proton spectroscopy in presence of eddy currents. *Magn Reson Med*. 1990;14(1):26-30. doi:10.1002/mrm.1910140104
44. Versluis MJ, Kan HE, van Buchem MA, Webb AG. Improved signal to noise in proton spectroscopy of the human calf muscle at 7 T using localized B1 calibration. *Magn Reson Med*. 2010;63(1):207-211. doi:10.1002/mrm.22195
45. Simpson R, Devenyi GA, Jezzard P, Hennessy TJ, Near J. Advanced processing and simulation of MRS data using the FID appliance (FID-A)—an open source, MATLAB-based toolkit. *Magn Reson Med*. 2017;77(1):23-33. doi:10.1002/mrm.26091
46. Michaelis T, Helms G, Frahm J. Metabolic alterations in brain autopsies: proton NMR identification of free glycerol. *NMR Biomed*. 1996;9(3):121-124. doi:10.1002/(SICI)1099-1492(199605)9:33.0.CO;2-F
47. Dong Z, Milak MS, Mann JJ. Proton magnetic resonance spectroscopy thermometry: impact of separately acquired full water or partially suppressed water data on quantification and measurement error. *NMR Biomed*. 2022;35(6):e4681. doi:10.1002/nbm.4681
48. Govindaraju V, Young K, Maudsley AA. Proton NMR chemical shifts and coupling constants for brain metabolites. *NMR Biomed*. 2000;13(3):129-153. doi:10.1002/1099-1492(200005)13:33.0.CO;2-V
49. Zoelch N, Heimer J, Richter H, Thali MJ, Gascho D. Finding the optimal temperature calibration for postmortem MRS thermometry in forensic medicine. In: *Proceedings of the ISMRM Annual Meeting & Exhibition*. International Society for Magnetic Resonance in Medicine; 2022. 2172
50. Li W, Chang Y, Han L, et al. Trimethylamine in postmortem tissues as a predictor of postmortem interval estimation using the GC method. *Leg Med*. 2018;35:80-85. doi:10.1016/j.legalmed.2018.09.011
51. Craciun S, Balskus EP. Microbial conversion of choline to trimethylamine requires a glycol radical enzyme. *Proc Natl Acad Sci U S A*. 2012;109(52):21307-21312. doi:10.1073/pnas.1215689109
52. Yablonskiy DA, Luo J, Sukstanskii AL, Iyer A, Cross AH. Biophysical mechanisms of MRI signal frequency contrast in multiple sclerosis. *Proc Natl Acad Sci U S A*. 2012;109(35):14212-14217. doi:10.1073/pnas.1206037109
53. Monoranu CM, Apfelbacher M, Grünblatt E, et al. pH measurement as quality control on human post mortem brain tissue: a study of the BrainNet Europe consortium. *Neuropathol Appl Neurobiol*. 2009;35(3):329-337. doi:10.1111/j.1365-2990.2008.01003a.x
54. Tredwell GD, Bundy JG, De Iorio M, Ebbels TM. Modelling the acid/base ^1H NMR chemical shift limits of metabolites in human urine. *Metabolomics*. 2016;12(10):152. doi:10.1007/s11306-016-1101-y
55. Dong Z, Kantrowitz JT, Mann JJ. Improving the reproducibility of proton magnetic resonance spectroscopy brain thermometry: theoretical and empirical approaches. *NMR Biomed*. 2022;35(9):e4749. doi:10.1002/nbm.4749
56. Heimer J, Gascho D, Madea B, et al. Comparison of the beta-hydroxybutyrate, glucose, and lactate concentrations derived from postmortem proton magnetic resonance spectroscopy and biochemical analysis for the diagnosis of fatal metabolic disorders. *Int J Leg Med*. 2020;134(2):1-10. doi:10.1007/s00414-019-02235-6
57. Berger C, Bauer M, Scheurer E, Lenz C. Temperature correction of post mortem quantitative magnetic resonance imaging using real-time forehead temperature acquisitions. *Forensic Sci Int*. 2023;348:111738. doi:10.1016/j.forsciint.2023.111738
58. Berger C, Birkel C, Bauer M, Scheurer E, Lenz C. Technical note: quantitative optimization of the FLAIR sequence in post mortem magnetic resonance imaging. *Forensic Sci Int*. 2022;341:111494. doi:10.1016/j.forsciint.2022.111494
59. Landheer K, Schulte RF, Treacy MS, Swanberg KM, Juchem C. Theoretical description of modern ^1H in vivo magnetic resonance spectroscopic pulse sequences. *J Magn Reson Imaging*. 2020;51(4):1008-1029. doi:10.1002/jmri.26846

SUPPORTING INFORMATION

Additional supporting information can be found online in the Supporting Information section at the end of this article.

How to cite this article: Zoelch N, Heimer J, Richter H, et al. In situ temperature determination using magnetic resonance spectroscopy thermometry for noninvasive postmortem examinations. *NMR in Biomedicine*. 2024;e5171. doi:10.1002/nbm.5171